Journal of Advanced Research 37 (2022) 119–131

Contents lists available at ScienceDirect

Journal of Advanced Research

journal homepage: www.elsevier.com/locate/jare

O-GlcNAc modification mediates aquaporin 3 to coordinate endometrial cell glycolysis and affects embryo implantation

Hongshuo Zhang [a], Jia Qi [a], Jingyuan Pei [a], Man Zhang [a], Yuhong Shang [b], Zhen Li [a], Yufei Wang [a], Jinqiu Guo [a], Kaiqi Sun [c], Jianhui Fan [a], Linlin Sui [a], Yuefei Xu [a], Li Kong [d,*], Ying Kong [a,*]

[a] *Department of Biochemistry and Molecular Biology, College of Basic Medical Sciences, Dalian Medical University, Dalian 116044, Liaoning, China*
[b] *Department of Gynecology, First Affiliated Hospital of Dalian Medical University, Dalian 116021, Liaoning, China*
[c] *Department of Clinical Medicine, Dalian Medical University, Dalian 116044, Liaoning, China*
[d] *Department Histology and Embryology, College of Basic Medical Sciences, Dalian Medical University, Dalian 116044, Liaoning, China*

HIGHLIGHTS

- *O*-GlcNAcylation affects endometrial cell physiological changes and implantation
- *O*-GlcNAcylation causes glucose metabolism to be redirected to PPP and HBP
- *O*-GlcNAcylation-mediated AQP3 provides compensation for glycolysis
- *O*-GlcNAcylation of Sp1 promotes the expression of AQP3
- OO-GlcNAcylation of Sp1 affects its stability

GRAPHICAL ABSTRACT

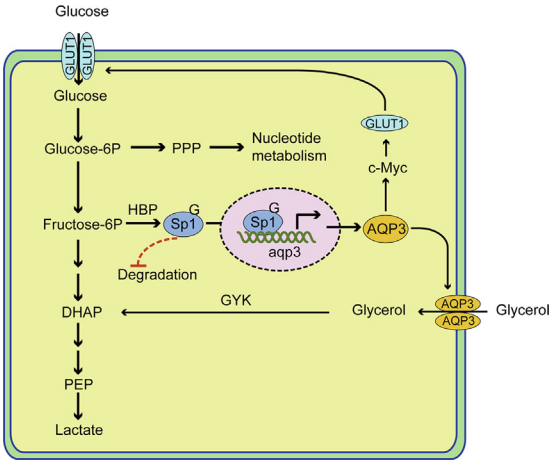

ARTICLE INFO

Article history:
Received 10 January 2021
Revised 28 June 2021
Accepted 28 June 2021
Available online 30 June 2021

Keywords:
O-GlcNAc modification
Glycolytic metabolism
AQP3
Implantation
SP1

ABSTRACT

Introduction: *O*-linked β-D-N-acetylglucosamine (*O*-GlcNAc) modification is a post-translational modification in which a single *O*-GlcNAc is added to serine or threonine residues in nuclear, cytoplasmic, and mitochondrial proteins, and is involved in a variety of physiological processes.
Objectives: In the present study, the role of *O*-GlcNAcylation in embryo implantation was evaluated. Furthermore, whether *O*-GlcNAcylation is involved in orchestrating glucose metabolism to influence endometrial cell physiological functions was investigated.
Methods: Different endometrial tissues were detected using immunohistochemistry. Pregnant mouse models were established to verify molecular expression. *O*-GlcNAc transferase and aquaporin 3 (AQP3) knockdown were used to detect embryo implantation efficiency *in vitro* and *in vivo*. Western blotting and immunofluorescence were used to detect protein expression and stability. Dual luciferase reporter assay and chromatin immunoprecipitation (ChIP) were used to verify the binding transcription factor. Glycolysis was detected using bioenergy analyzer, and metabolites were analyzed using isotope 13C-labeled LC-MS. Metabolic-related genes were determined using RNA sequencing.

Peer review under responsibility of Cairo University.
* Corresponding authors.
E-mail addresses: kongli@dmu.edu.cn (L. Kong), yingkong@dmu.edu.cn (Y. Kong).

https://doi.org/10.1016/j.jare.2021.06.022
2090-1232/

Results: Activation of endometrial hexosamine biosynthetic pathway (HBP) caused elevated *O*-GlcNAcylation during the window of implantation, affecting endometrial cell function and embryo implantation. Specifically, elevated *O*-GlcNAcylation increased glucose uptake *via* glucose transporter 1 (GLUT1) leading to glucose metabolic flow into the pentose phosphate pathways and HBP, which regulate the metabolic reprogramming of endometrial cells. Furthermore, *O*-GlcNAcylation mediated the intracellular transport of glycerol to support and compensate for glycolysis through regulation of AQP3. Unexpectedly, elevated AQP3 also increased glucose uptake *via* GLUT1. These processes maintained higher metabolic requirements for endometrial physiology. Furthermore, the transcription factor SP1 specifically bound to the AQP3 promoter region, and *O*-GlcNAcylation of SP1 increased its stability and transcriptional regulation of AQP3 which is associated with *O*-GlcNAcylation of SP1.
Conclusion: Overall, *O*-GlcNAcylation regulated glucose metabolism in endometrial cells, and AQP3-mediated compensation provides new insights into the communication between glycolysis and *O*-GlcNAcylation.

Introduction

O-linked β-D-N-acetylglucosamine (*O*-GlcNAc) modification is one of the most abundant post-translational modifications in eukaryotic cells and is believed to consist of the addition of a single *O*-GlcNAc to serine or threonine residues of nuclear, cytoplasmic, and mitochondrial proteins [1]. To date, only two enzymes have been found responsible for the regulation of *O*-GlcNAcylation, *O*-GlcNAc transferase (OGT), catalyzing the addition of *O*-GlcNAc, and *O*-GlcNAcase (OGA), catalyzing the hydrolysis of *O*-GlcNAc. *O*-GlcNAcylation regulates multiple pathways by affecting protein transcription, localization, interaction, activity, and degradation, thereby regulating cellular physiology rapidly and reversibly by sensing a wide range of signals [2]. Notably, most proteins that can be modified by *O*-GlcNAc are also thought to undergo phosphorylation, and in many cases, extensive cross-talk between the two modifications regulates protein function [3]. Furthermore, although abnormal *O*-GlcNAcylation of key proteins has been shown to occur in a variety of diseases [4], the role of *O*-GlcNAc modification in pregnancy has rarely been described.

Mammalian embryo implantation refers to the process in which the blastocyst becomes implanted in the endometrium through a series of events such as recognition, localization, adhesion, and crossing the basement membrane. These series of complex events occur in a specific period called the window of implantation. The endometrial conditions required for the successful completion of this process mainly consist of the appropriate differentiation of the endometrium at the right time. The endometrium undergoes profound cellular and biochemical changes, from being proliferative to secretory, in the pre-implantation of the embryo, which leads to the endometrium entering a receptive state [5]. Decidualization of endometrial stromal cells further supports the maintenance of pregnancy [6]. Human pregnancy efficiency is relatively low and 75% of pregnancy failures are associated with defects that occur during *peri*-implantation [7]. Evidence indicates that glucose metabolism plays an important role in the *peri*-implantation of humans and rodents [8,9]. Because the precursor of *O*-GlcNAcylation, UDP-GlcNAc, connects the metabolic pathways of glucose, fatty acids, nucleic acids, and nitrogen, *O*-GlcNAcylation as a nutrient sensor appears crucial for physiological and metabolic processes such as cell growth, survival, sensing nutritional status, and integration of multiple signaling pathways [10]. However, how the *O*-GlcNAcylation regulates the signaling pathway that coordinates metabolism to affect endometrial physiology and to prepare for implantation remains unknown.

In the present study, *O*-GlcNAcylation was shown to have a regulatory effect on changes of endometrium physiological and implantation during the window of implantation. Increased GLUT1 promoted *O*-GlcNAcylation levels by the hexosamine biosynthetic pathway (HBP); elevated *O*-GlcNAcylation affected endometrial cell function and redirected glucose metabolic flow, shunting it to the pentose phosphate pathway (PPP) and HBP. In addition, increased glycolysis levels decreased the TCA cycle, and elevated ATP and lactate levels in endometrial tissue at the secretory phase increased the existence of Warburg-like glycolysis during the window of implantation. This increased glycolysis level can be achieved by increasing glucose uptake through the *O*-GlcNAcylation regulation of GLUT1, and the regulation of aquaporin 3 (AQP3) by *O*-GlcNAcylation mediates the intracellular transport of glycerol to compensate for increased glycolysis. Furthermore, the *O*-GlcNAcylation of SP1 regulated AQP3. Conversely, this indicated that metabolic changes provide cells with possible biosynthetic intermediates such as nucleotides as well as energy supply and overall response to physiological changes in the endometrium. In general, the present study results, at least partly explain the adverse pregnancy outcomes observed in metabolic disorders and provides a reference for understanding metabolic mechanisms within the endometrium during implantation.

Materials and methods

Samples

Human endometrium samples were obtained from the First Affiliated Hospital of Dalian Medical University. Clinical sample information was provided in table S1. The pathology of the samples was verified by pathologists through hematoxylin-eosin (HE) staining.

Mice experiments

Adult female ICR mice were obtained from the Dalian Medical University animal center. First, mice were mated in cages in the evening at a female: male of 2:1. Subsequently, the next morning female mice were checked for the formation of a vaginal plug. If a vaginal plug was present, this was defined as the first day (D1) of the mating. Uterine tissues were collected during D1-D5 (*peri*-implantation). The implantation efficiency was determined by uterine horn injection, as described in previous studies [11,12]. On D3, the uterine horn injection of OGT, AQP3, GLUT1 siRNA (100 pmol and 5 μL Lipo2000 in 20 μL normal saline) was performed, while the other side of the uterus was injected with normal saline. On D7, the mice were killed by anesthetic and the number of embryos examined and counted. The interference sequences were in table S2.

Ethics statement

All experiments involving animals were approved by the Animal Ethics committee of the Dalian Medical University (AEE21033). Informed consent was obtained from patients for using their samples in this study, and this project was approved by the Ethics Committee of First Affiliated Hospital of Dalian Medical University (YJ-KY-FB-2021–13).

Plasmids

SP1 and AQP3 over-expression (over-AQP3/SP1) plasmids, short hairpin (sh)AQP3 plasmid, and an empty vector (negative control, NC) plasmid were purchased from Geneopoeia company (Rockville, MD, USA). Six putative *O*-GlcNAcylation sites (S491, S612, T640, S641, S698, and S702) of SP1 were mutated to alanine (enhanced green fluorescent protein (eGFP)-SP1-MT) by Tongyong Company (Chuzhou, China), with WT the control group (eGFP-SP1-WT). The full-length cDNA of SP1 (785aa) was cloned into a pcDNA3.1 (-) vector with an eGFP tag. All constructs were confirmed by DNA sequencing.

Cell culture

HEC-1A, RL95-2, Ishikawa, JAR (as an embryo model) [13–15], and HeLa cell lines were purchased from the American Tissue Culture Collection. AN3-CA cell lines were purchased from Procell Life Science & Technology Co.,Ltd (Wuhan, China). HEC-1A cells were grown in McCoy's 5A, Ishikawa and JAR cells were grown in RPMI 1640, AN3-CA and HeLa cells were grown in DMEM medium (Thermo Fisher Scientific, Inc.). RL95-2 cells were grown in DMEM/F-12 medium containing 0.005 mg/mL insulin.

Knockdown by small interfering RNA

Cells were seeded in 35 mm plates (1×10^6 cells), and 24 h later, were infected with 100 mM of siRNA targeting OGT, OGA, SP1, E2F1, NF-κB1 ((si)SP1, (si)E2F1, (si)NF-κB1 sequences have been validated in our other studies), and negative control (scrambled sequence) used 5 μL Lipofectamine 2000 (Invitrogen, USA). The interference sequences were in table S3.

Cell proliferation assay

The Cell Counting Kit-8 (CCK-8) assay (APExBIO, Houston, TX, USA) detected cell proliferation and viability according to the manufacturer's instructions.

Cell invasion, migration, and in the vitro adhesion assay

Invasion and migration assays were conducted in Transwell, with or without Matrigel matrix (BD Biosciences, USA), respectively. Briefly, the number of cells invading (with Matrigel) or migrating to (without Matrigel) the filter membrane bottom was observed. For the adhesion assay, JAR cells were pretreated with CellTraceTM CFSE (Invitrogen, Carlsbad, CA, USA) and then resuspended and added to a treated culture plate containing HEC-1A/RL95-2 cell monolayer, which was gently shaken (40 rpm, for spheroids) for 1 h at 37C, and attached cells were observed.

Cellular bioenergetics analysis

The extracellular acidification rate (ECAR), an indicator of glycolysis, and oxygen consumption rate (OCR), an important metric for mitochondrial function, were measured with a Seahorse Biosciences XF Analyzer (Seahorse Bioscience Inc., USA). An XF Glycolysis Stress Test Kit was used to measure glycolytic capacity (ECAR, Seahorse Bioscience Inc.). Basal OCR was also determined.

Glucose uptake, lactate, ATP, glycerol, and glycogen assays

For the glucose uptake assay, 2-NBDG (APExBIO) was used to incubate the cells in the glucose-free medium. Images were then acquired using a fluorescence microscope. Intracellular lactate and ATP levels were determined using a CheKine™ Lactate Assay Kit (Abbkine, Wuhan, China), and ATP detection Assay Kit (Solarbio, Beijing, China), respectively. Glycerol levels of intracellular and tissue were determined using a Glycerol Assay Kit (Nanjing Jiancheng, Nanjing, China). Periodic Acid Schiff (PAS) reagent (Nanjing Jiancheng) was used to detect the Glycogen content according to the manufacturer's protocol.

Isotope carbon metabolic tracing

Cells were cultured in a medium containing uniformly labeled U-13C6-glucose. After 24 h, samples (5×10^6 cells/sample) were washed with ice-cold PBS, 1 ml of methanol–water (4:1, V/V; pre-frozen at −80C for 4–6 h) added, and samples incubated at −80C for 20 min. The cells were then collected and stored at −80C. Metabolites were detected and analyzed by LipidALL Technologies Co., Ltd. (Changzhou, China).

Transcriptome sequencing and analysis

Transcriptome analysis was performed by Novogene Technology Co., Ltd. (Beijing, China). Illumina sequencing was then performed after library pooling. The number of reads covered from initiation to termination of each gene (including the new predictive gene) was counted using Subread software. HISAT2 software was used to accurately compare Clean Reads with an Hg19 human genome to obtain the location information of Reads. Normalization was performed on the original Readcount to screen genes whose expression levels were significantly in different states.

Immunoprecipitation (IP) and immunoblotting

Proteins were extracted on ice with radioimmunoprecipitation buffer from 1 to 5×10^6 cells (Transgene, Beijing, China). For IP, lysates were incubated with the appropriate antibody: anti-SP1 (Proteintech, Wuhan, China). Subsequently, Protein A/G –agarose (Santa Cruz Biotechnology. Inc, USA) was added to lysates for 4 h to IP the target protein. For immunoblotting, protein samples or the IP were separated by 10% SDS-PAGE and transferred to nitrocellulose membranes (Millipore, Burlington, USA). The membranes were incubated with the following antibodies: *O*-GlcNAc (1:1000, ab2739, RL2, Abcam, Cambridge, MA, USA), OGT (1:1000, 11576–2-AP, Proteintech, Wuhan, China), OGA (1:1000, 14711–1-AP, Proteintech), AQP3 (1:1000, ab125219, Abcam), beta-actin (1:1000, 20536–1-AP, Proteintech), GLUT1 (1:1000, 66290–1-Ig, Proteintech), c-Myc (1:2000, 10828–1-AP, Proteintech), SP1 (1:2000, 21962–1-AP, Proteintech), Lamin B1 (1:2000, 12987–1-AP, Proteintech), at 4 °C overnight, respectively. Then, the membranes were incubated with horseradish peroxidase-conjugated secondary antibody (Proteintech) for 1 h at room temperature and visualized using a chemiluminescent substrate (Invitrogen, USA) by an Image Lab detection system (Bio-Rad, USA).

Quantitative polymerase chain reaction (PCR)

RNA Extraction Kit (Takara, Japan) was used to total RNA isolation. A reverse-transcription kit (Takara) was used to synthesis the

cDNAs, and the ABI StepOne Real-time PCR system (Applied BioSystems, USA) analyzed the target genes by real-time PCR. Fold changes were calculated from raw data using the $2^{-\triangle\triangle CT}$ method. The primer sequences were in table S4.

Immunohistochemistry (IHC)

Paraffin sections of tissues were deparaffinized in xylene. After endogenous peroxidase activity was quenched by hydrogen peroxide, the paraffin sections were stained with specific antibodies: *O*-GlcNAc (1:100, ab2739, RL2, Abcam), GLUT1 (1:100, 66290–1-Ig, Proteintech), GFAT (1:100, 14132–1-AP, Proteintech), or GYK (1:100, 13360–1-AP, Proteintech). Immunodetection was carried out with biotinylated IgG (ZSGB-Biotechnology Co., Beijing, China), followed by incubation with horseradish peroxidase-labeled streptavidin solution. Finally, the color reactants were developed with diaminobenzidine.

Luciferase reporter assay

The AQP3 promoter-luciferase reporter system was constructed by ligating a DNA fragment encoding the human AQP3 promoter into pGL3-basic (Promega, Madison, WI, USA). A dual-luciferase reporter assay system (Promega) was used to measure the luciferase activities in cell lysates after cells were co-transfected with the AQP3 promoter-luciferase gene, or siSP1 or siE2F1 small interfering RNAs or an SP1-overexpressing vector. Renilla luciferase was used for the normalized of Luciferase values.

Chromatin immunoprecipitation (ChIP) assay

HeLa cells were crosslinked with 1% formaldehyde and then were sonicated in lysis buffer. The sonicated lysates were incubated with normal IgG, or SP1 antibody overnight at 4℃ and were IP with protein A/G agarose. Samples were reverse crosslinked at 65℃ for 4 h, and the IP DNA fragments were extracted with phenol/chloroform/isoamyl alcohol (25:24:1). Agarose electrophoresis was used for the analysis of PCR products. The AQP3-S1 primer sequences were as follows: forward: 5'-TCCATGCCCG CAGCTCCCTCCA-3'; reverse: 5'-CTCCAGCGCTGGTGGCTCCCTTTA-3'.

Immunofluorescence (IF) staining

Cells were fixed in 4% paraformaldehyde and were permeabilized using 0.1% Triton X-100, followed by anti-*O*-GlcNAc (1:100, ab2739, RL2, Abcam), anti-SP1 (1:100, 21962–1-AP, Proteintech) incubation overnight at 4 °C. Then cells were incubated with CL594-conjugated anti-rabbit (1:500, SA00013-4, Proteintech) or CL488-conjugated anti-mouse IgG (1:500, SA00013-1, Proteintech) secondary antibodies, and cell nuclei were stained with DAPI. Images were acquired by using an Olympus BX51 immunofluorescence microscope.

Statistical analysis

All data are presented as mean ± standard deviations. The statistical analyses were performed using Student's *t*-test and one-way ANOVA by GraphPad Prism 8.0 (GraphPad Software). A value of $P < 0.05$ was considered statistically significant. Experiments were repeated three or more times.

Results

O-GlcNAc modification is important for cell function and pregnancy outcomes

To investigate the possible role of *O*-GlcNAc modification in pregnancy, samples of human endometrium were collected and the proliferative and secretory phases identified using hematoxylin and eosin (H&E) staining (Fig. S1A). Immunohistochemistry results showed higher levels of *O*-GlcNAc modification in the secretory phase (Fig. 1A) and mainly localized in glandular epithelium. Based on *in vitro* cell models [13–15] showing *O*-GlcNAc modification levels were higher in RL95-2 and Ishikawa cells than in HEC-1A and AN3-CA cells (Fig. 1B), we selected commonly used HEC-1A (as non-receptive endometrial epithelial cells) and RL95-2 (as receptive endometrial epithelial cells) cells [13–15]. Subsequently, *O*-GlcNAcylation levels were modulated using small interfering (si) RNAs, siOGT and siOGA. Verification results are shown in Figure S1B–D, thus, siOGT3 and siOGA3 were used for subsequent experiments. Furthermore, regulation of *O*-GlcNAcylation levels significantly affected cell proliferation (Fig. 1C), migration (Fig. 1D), invasion (Fig. 1E), and adhesion (Fig. 1F). To analyze the effects of *O*-GlcNAcylation depletion on pregnancy outcomes *in vivo*, negative control (NC, scrambled siRNA) or siOGT were injected into the uterine horn and embryo implantation evaluated. Results showed the implantation rate was significantly lower, approximately 0.38-fold, than in the control group (Fig. 1G). In addition, the OGT mRNA level in the endometrial tissue of spontaneous abortions was significantly lower than in induced abortions (Fig. 1H), which further indicated that *O*-GlcNAcylation might be involved in endometrial changes during the embryo implantation process.

Elevated GLUT1 increases *O*-GlcNAcylation through HBP during the window of implantation

O-GlcNAcylation uses UDP-GlcNAc as a substrate in the HBP, a branch of glucose metabolism [16]. In the present study, GLUT1 expression was increased in the secretory phase (Fig. 2A) and mainly located in glandular epithelium and stroma. In addition, the accumulation of glycogen in the endometrium indicated metabolic changes (Fig. S2A). Considering the importance of glucose for implantation, we altered the glucose concentration and found that 15 mM and 25 mM glucose increased GLUT1, *O*-GlcNAcylation, and OGT levels compared with the high osmotic group (5.5 mM glucose + 19.5 mM mannose), however, significant change was not observed in OGA (Fig. 2B). We hypothesized this effect was mediated by the HBP, thus, the cells were then treated with 6-diazo-5-oxo-l-norleucine (DON) [17], an inhibitor of the key enzyme glutamine fructose-6-phosphate aminotransferase (GFAT), and glucosamine ($GlcNH_2$), a downstream substance of GFAT, as activators [18]. Results showed that DON hindered *O*-GlcNAcylation levels by inhibiting the HBP pathway (Fig. 2C), and $GlcNH_2$ increased *O*-GlcNAcylation levels in a concentration-dependent manner (Fig. 2D). Thus, we speculated that elevated levels of secretory *O*-GlcNAc modification was caused by GLUT1-mediated HBP. This hypothesis was confirmed by elevated GFAT in the human endometrium (Fig. 2A). Furthermore, we developed pregnant mouse models and validated the uterine window of implantation using Hoxa10 (Fig. 2E), a promising candidate for measuring endometrial receptivity [19,20]. Results showed the expression of GLUT1, GFAT (Fig. 2F), and glycogen (Fig. S2B) was increased during D3–D5.

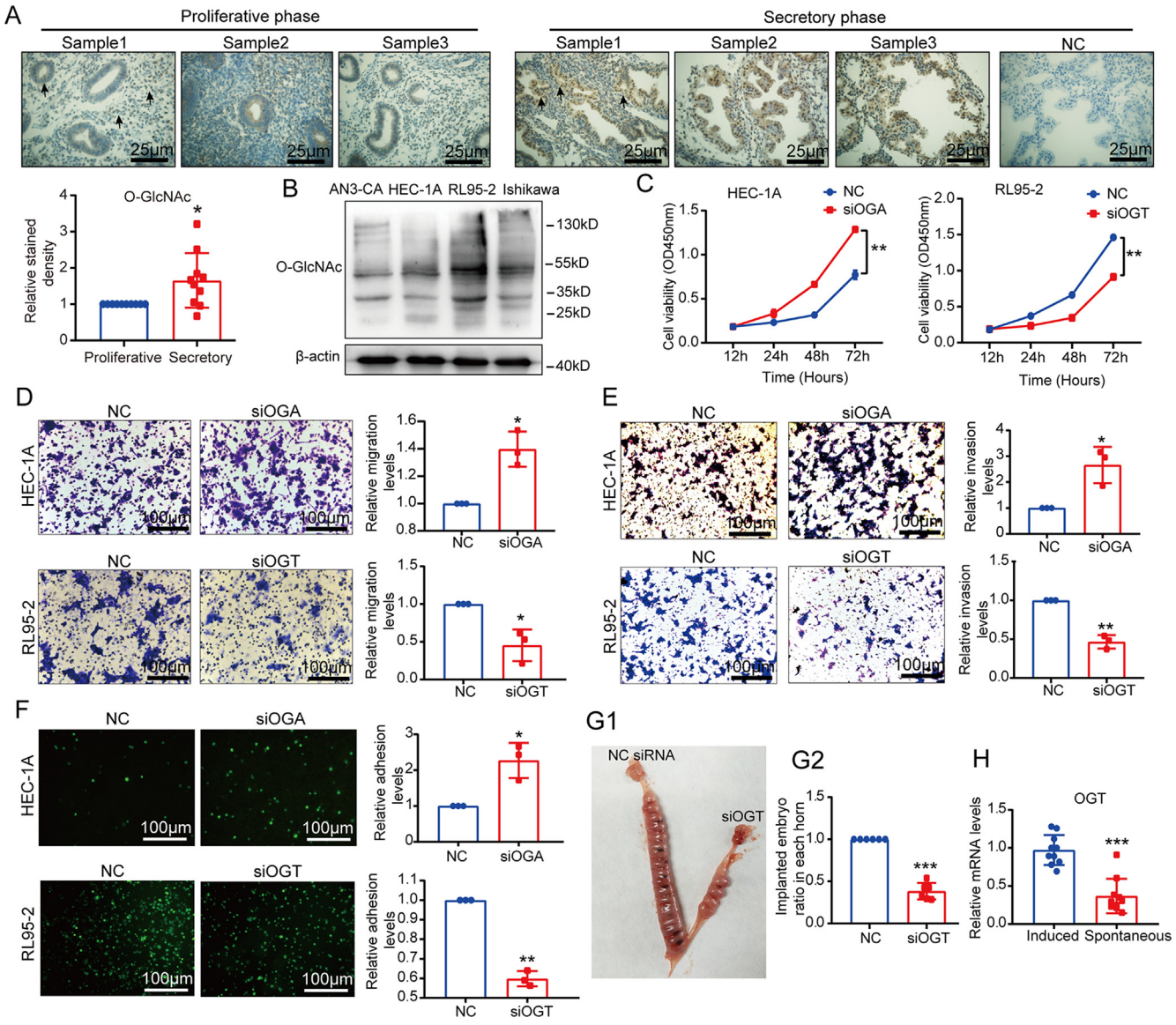

Fig. 1. *O*-GlcNAcylation affects cell function and pregnancy outcomes. (A). *O*-GlcNAcylation levels in human endometrial tissue were analyzed by IHC (n = 20; scale bar = 25 μm). (B). WB analysis of *O*-GlcNAcylation levels in HEC-1A, AN3-CA, RL95-2 and Ishikawa cells. (C). Cell proliferation assay of siOGA-treated HEC-1A and siOGT-treated RL95-2 cells by CCK-8 kit (n = 3). (D-E). Cell migration (D) and invasion (E) in siOGA-treated HEC-1A and siOGT-treated RL95-2 cells by Transwell assay (scale bar = 100 μm; n = 3). (F). The adhesion assays of JAR cells to siOGA-treated HEC-1A and siOGT-treated RL95-2 cells (scale bar = 100 μm; n = 3). (G1). Effect of OGT knockdown on implantation rate with a photograph showing typical mouse uterus at D7 of pregnancy. (G2). The implanted embryo ratio in each horn was analyzed (n = 6). (H). The qPCR analysis of OGT mRNA in human endometrial tissue samples from induced abortions and spontaneous abortions (normalized to β-actin, n = 10). Error bars represent the mean ± standard deviation. Student's *t*-test, *P < 0.05, **P < 0.01, ***P < 0.001.

O-GlcNAcylation regulates metabolic reprogramming

We hypothesized that *O*-GlcNAcylation can be used as an important regulator of endometrial glucose metabolism during embryo implantation. To test this hypothesis, extracellular acidification rate (ECAR, approximate glycolysis) was measured. As expected, ECAR was affected by *O*-GlcNAcylation (Fig. S3A). Furthermore, alloxan [21] and PUGNAc [22], inhibitors of OGT and OGA, respectively, affected cellular *O*-GlcNAcylation levels (Fig. S3B) and regulated ECAR (Fig. 3A). Notably, downregulation of *O*-GlcNAcylation increased the oxygen consumption rate (OCR) (approximate aerobic respiration) in cells (Fig. S3C). Potentially, *O*-GlcNAcylation acts as an induction regulator to control the balance between glycolysis and the TCA cycle. To further confirm the changes in glycolysis, the effect of *O*-GlcNAcylation on isotope 13C-labeled metabolites was analyzed using LC-MS. The metabolic profiles of PUGNAc-treated cells showed a general increase in glycolysis, PPP, and HBP metabolites (Fig. 3B) and a decrease in TCA cycle metabolites (Fig. 3C), a typical Warburg effect. The regulation of *O*-GlcNAcylation by alloxan- and PUGNAc-treated cells also affected the lactate levels (Fig. S3D). In addition, the lactate (Fig. 3D) and ATP (Fig. 3E) levels were increased in the secretory phase of human endometrial tissue. These results indicated that *O*-GlcNAcylation might participate in the endometrial change by regulating glycolytic metabolism.

O-GlcNAcylation regulates GLUT1 and AQP3 based on transcriptome analysis

To study the main regulatory pathways inhibiting OGT and explain the regulation of *O*-GlcNAcylation in metabolic reprogramming, transcriptome-sequencing analysis of siOGT-treated cells

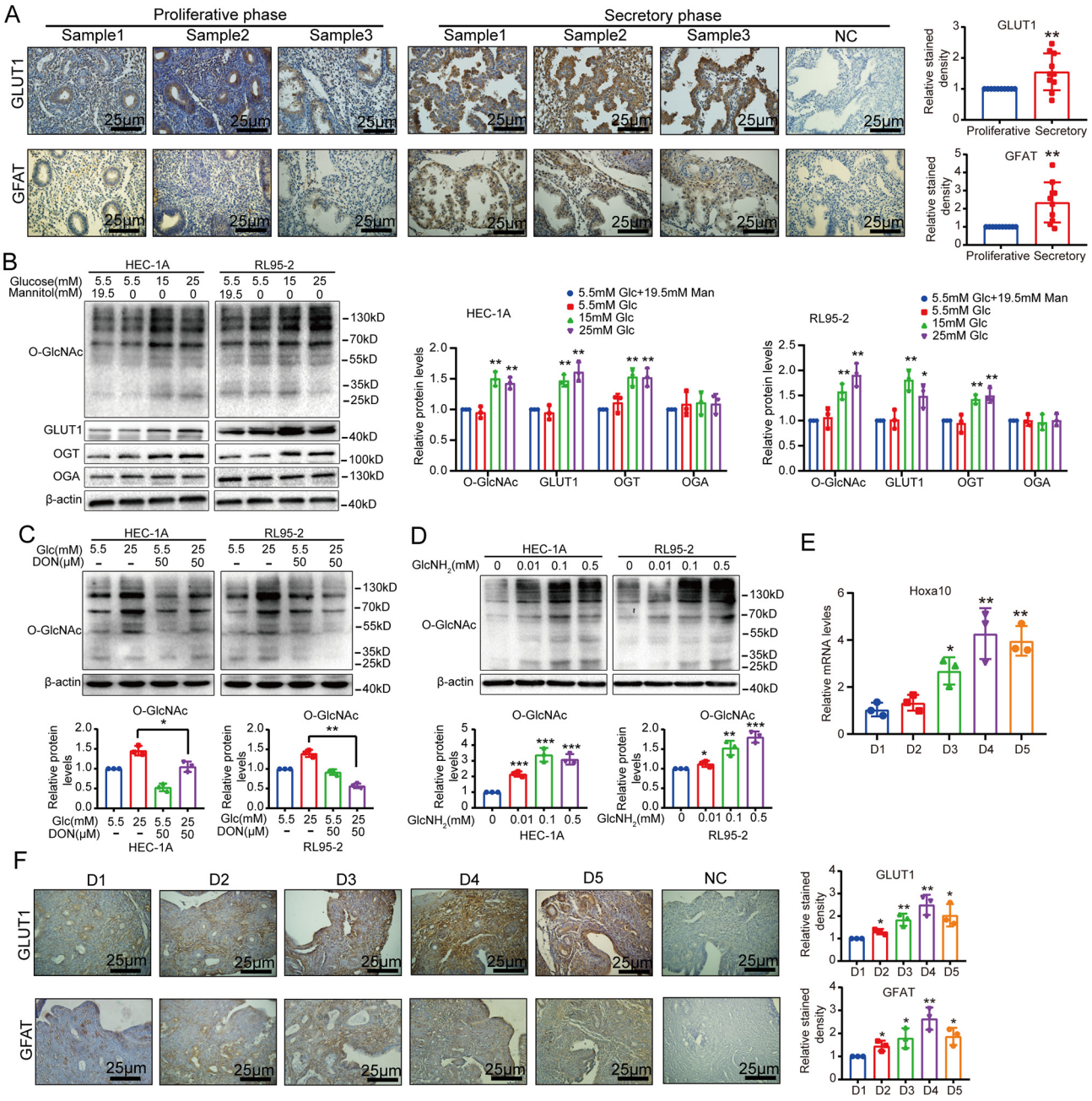

Fig. 2. GLUT1 and HBP are up-regulated during the "window of implantation". (A). GLUT1, GFAT in human endometrial tissues were analyzed by IHC (n = 20; scale bar = 25 μm). (B). HEC-1A and RL95-2 cells treated with glucose (5.5 mM, 15 mM, 25 mM, 5.5 mM glucose + 19.5 mM mannitol as high osmotic control) for 48 h. The levels of *O*-GlcNAcylation, GLUT1, OGA, and OGT were analyzed by WB (n = 3; *vs.5.5 mM Glc + 19.5 mM Man). (C). HEC-1A and RL95-2 cells were exposed to 5.5 mM, 25 mM glucose, with or without DON (50 mM) for 48 h. WB was used to analyze *O*-GlcNAcylation levels (n = 3). (D). HEC-1A and RL95-2 cells were treated at different glucosamine concentrations (0.01, 0.1, 0.5 mM) for 48 h. WB was used to analyze *O*-GlcNAcylation levels (n = 3; *vs.0 mM $GlcNH_2$). (E). The qPCR analysis of Hoxa10 mRNA in the uteri of mouse D1–D5 (normalized by Gapdh; n = 3; *vs.D1). (G). IHC analysis of GLUT1, GFAT in the uteri of mouse D1–D5 (Scale bar = 25 μm; n = 3). Error bars represent the mean ± standard deviation. Student's *t*-test, One-way ANOVA, *P < 0.05, **P < 0.01, ***P < 0.001.

was performed. Among the 26,429 identified transcripts, 1,587 were upregulated and 2,266 were downregulated (Fig. 3F). To determine whether these genes were associated with metabolic reprogramming, Gene Ontology (GO) analysis was performed. GO results showed that most of the regulated genes belonged to the categories of ribosomal metabolism, nucleotide biosynthesis, energy metabolite biosynthesis, and protein stabilization (Fig. S4A). The enrichment analysis using the Kyoto Encyclopedia of Genes and Genomes (KEGG) pathways showed that regulated genes were involved in the pathway of central carbon metabolism (Fig. 3G), the first step in glucose utilization. Therefore, the GLUTs (encoded by the SLC2 gene), which are responsible for glucose intake into the cell, were further investigated. Among the SLC2 family transcripts, SLC2A1 showed the most significant downregulation based on sequencing (Fig. 3H), and the regulatory effects of *O*-GlcNAcylation on GLUT1 were verified based on siRNAs (Fig. S4B).

O-GlcNAc modification of key enzymes (PFK1, PKM2) of glycolysis has been documented to inhibit their activity [23,24]. In the present study, elevated *O*-GlcNAcylation increased the glycolysis level which may be due to the effect of *O*-GlcNAcylation on GLUT1 (Fig. 3H). In previous studies, hypoxia-inducible factor-1a and c-

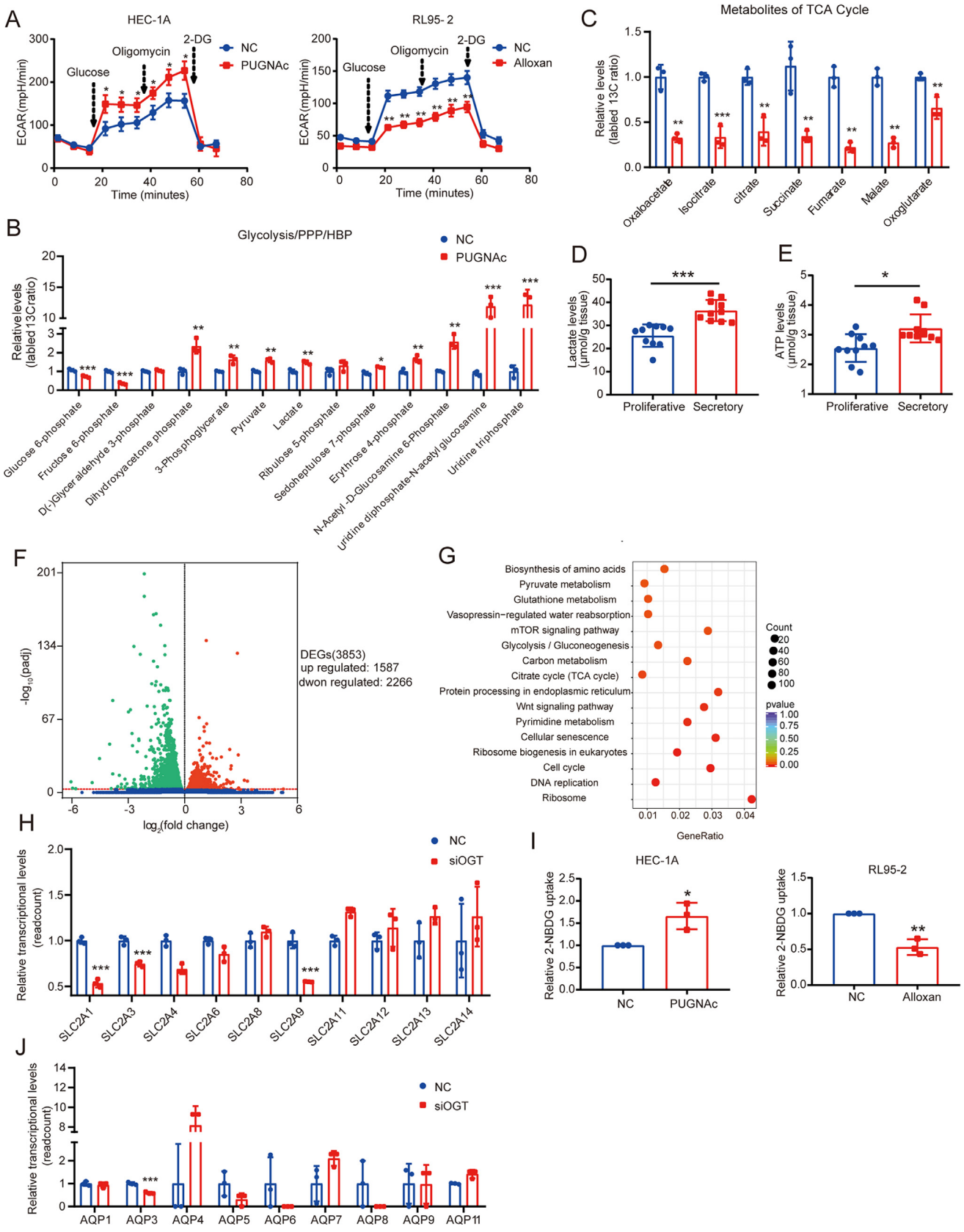

Fig. 3. Modulation of *O*-GlcNAcylation levels affects cellular metabolism. (A). The ECAR in PUGNAc-treated HEC-1A cells and alloxan-treated RL95-2 cells (n = 3). (B-C). LC–MS analysis was used to determine the levels of 13C-labeled glycolysis, PPP, HBP metabolites (B), and TCA cycle intermediates (C) in PUGNAc-treated HEC-1A cells (n = 3). (D-E). Lactate (D), and ATP (E) levels were measured in human endometrial tissues (n = 20). (F). Volcano map shows differentially expressed genes in siOGT-treated RL95-2 cells (padj < 0.001). (G). KEGG analysis of the pathways of significant gene enrichment in siOGT-treated RL95-2 cells (P < 0.05). (H). Relative transcriptional levels of SLC2 family genes detected in siOGT-treated RL95-2 cells (n = 3; *vs.NC). (I). 2-NBDG fluorescent glucose uptake assays in PUGNAc-treated HEC-1A cells and alloxan-treated RL95-2 cells (n = 3). (J). Relative transcriptional levels of AQP family genes detected in siOGT-treated RL95-2 cells (n = 3; *vs.NC). Error bars represent the mean ± standard deviation. Student's *t*-test, *P < 0.05, **P < 0.01, ***P < 0.001.

Myc were shown to mediate GLUT1 expression [23,25]. The regulation of GLUT1 by *O*-GlcNAcylation may be achieved through c-Myc (Fig. S4C). Furthermore, alloxan and PUGNAc regulated cellular glucose uptake (Fig. 3I). As expected, GLUT1 deficiency reduced glycolysis levels (Fig. S4D) and affected the implantation ratio *in vivo* when injecting siRNA into the uterine horn, which was demonstrated in our previous study [26]. In addition, evidence exists that AQPs (which are involved in the transport of small molecular substances such as water and glycerol) participate in energy metabolism and the proliferation of tissue cells by mediating glycerol transport [27–29]. In the present study, among the AQP family members, only AQP3 was significantly downregulated based on sequencing (Fig. 3J), which was confirmed using siRNAs (Fig. S4B). These results indicated that AQP3 may also be involved in the regulation of glycolysis.

AQP3 provides compensation for glycolytic metabolism

In comparison, glucose and activation or inhibition of the HBP pathway affected AQP3 expression (Fig. S5A, B), indicating that AQP3 was associated with glucose metabolism. Glycerol is also used as an important intermediate for glucose and lipid metabolism. Notably, the glycerol content was increased in the secretory phase of human endometrial tissue (Fig. 4A). To further determine the effects of AQP3 on glycolysis and the role of glycerol, glycerol was added to the cell medium. Regulation of *O*-GlcNAcylation affected the intracellular glycerol content (Fig. 4B), indicating that glycerol may enter the cell *via* AQP3. Furthermore, the AQP3 expression in RL95-2 cells was higher than in HEC-1A cells (Fig. 4C). The ECAR measurement results revealed that glycerol increased the glycolysis level, indicating that glycerol supported glycolysis (Fig. 4D). In addition, glycerol kinase (GYK) expression in the secretory phase of endometrial tissue was higher (Fig. 4E). Similar results were observed in pregnant mouse models during D3–D5 (Fig. 4F). Therefore, glycerol was transported into the cell *via* AQP3 and catalyzed by GYK to dihydroxyacetone phosphate to enter the glycolytic metabolic pathway.

Notably, glycerol also increased glycolysis levels in AQP3-downregulated RL95-2 cells (Fig. 4D), indicating this transport route is not unique and that other AQPs may be involved. In addition, the number of implanted embryos in the uteri of mice injected with AQP3 siRNA was slightly lower (approximately 0.7-fold) than in the control group (Fig. 4G). Therefore, AQP3 deletion likely affected normal embryo implantation but was not as detrimental to pregnancy outcome as OGT. However, the regulation of AQP3 also affected glycolysis levels without glycerol (Fig. 4D). Furthermore, AQP3 overexpression promoted 2-NBDG uptake and downregulation of AQP3 inhibited 2-NBDG uptake, indicating that modulation of AQP3 affects intracellular uptake of glucose (Fig. 4H) which may also be associated with c-Myc-mediated GLUT1. As expected, AQP3 regulation affected the c-Myc and GLUT1 expression (Fig. 4I). Overall, AQP3 supported glycolytic metabolism through intracellular transport of glycerol and increased GLUT1 expression, thus providing energy compensation for physiological changes of endometrial cells.

O-GlcNAcylation of SP1 promotes the AQP3 expression

The above evidence showed that AQP3 is involved in the effect of *O*-GlcNAcylation on glycolysis, and the specific mechanism by which *O*-GlcNAcylation regulates AQP3 requires further elucidation. Consequently, we predicted from multiple databases that SP1, E2F1, and nuclear factor (NF)-kB transcription factors might bind to the AQP3 promoter region. The downregulation of SP1 and E2F1 reduced AQP3 mRNA in HeLa cells (Fig. 5A). Subsequent dual-luciferase assays showed that downregulation of SP1 expression decreased fluorescence activity, however, downregulation of E2F1 did not cause a significant difference (Fig. 5B). The range of promoters that bound to SP1 (containing two specific binding sites, Fig. 5C) were identified and validated using chromatin immunoprecipitation (ChIP) experiments (Fig. 5D). In addition, high glucose increased SP1 and AQP3 expression, however, AQP3 was not significantly increased in the SP1-deficient group (Fig. S6A–C), further indicating that SP1 specifically binds to the AQP3 promoter region.

SP1 was modified by *O*-GlcNAc and was predicted to have multiple putative *O*-GlcNAcylation sites based on database analysis [17,30]. Our IP results confirmed that inhibitors affected SP1 *O*-GlcNAcylation levels (Fig. 5E). Alloxan inhibited the nuclear translocation of SP1, and this inhibition was restored by PUGNAc (Fig. 5F). Furthermore, similar results were observed when the cytoplasm and nuclei of cells were separated (Fig. 5G). To determine whether the *O*-GlcNAcylation of SP1 residues affects AQP3 expression, these residues were mutated to alanine to produce a SP1 mutant (eGFP)-SP1-MT plasmid (schematic, Fig. 5H). IP assays showed the *O*-GlcNAcylation levels of SP1-MT were reduced (Fig. 5I), and low residual *O*-GlcNAcylation levels were observed, which may be due to the endogenous SP1. Thus, endogenous SP1 was eliminated using siRNA before transfecting cells with SP1-MT and wild-type (WT) constructs. Results showed that SP1-MT reduced AQP3 expression compared with WT (Fig. 5J). In addition, similar results were obtained when HEC-1A cells were exposed to different glucose concentrations (Fig. S6D). Therefore, the *O*-GlcNAcylation of SP1 regulated AQP3 expression.

The O-GlcNAcylation of SP1 at the S491 site affects its stability

Inhibition or activation of the HBP also affected SP1 expression (Fig. S5A, B) likely due to *O*-GlcNAcylation of SP1. Downregulation of *O*-GlcNAcylation levels revealed a significant decrease in the SP1 protein level (Fig. 6A). Notably, the SP1 mRNA level was not consistent with its protein level (Fig. 6B). Furthermore, OGT knockdown-mediated SP1 downregulation was confirmed using alloxan, and PUGNAc upregulated SP1 protein level, demonstrating this is not an off-target effect (Fig. 6C). Therefore, *O*-GlcNAcylation likely regulates the stability of SP1 through a post-transcriptional mechanism. To detect whether the downregulation of *O*-GlcNAcylation levels alters the stability of SP1, OGT-knockdown RL95-2 cells were treated with cycloheximide (CHX) to inhibit protein synthesis, and residual SP1 was chased. SP1 protein levels decreased to approximately 80% in the control group and approximately 46% in the OGT downregulated group (Fig. 6D). Similar results showed the SP1 protein levels decreased from 83% in the control group to 34% in the alloxan-treated group (Fig. 6E).

The above results showed the importance of *O*-GlcNAc modification for maintaining SP1 stability. To explore the degradation pathway of SP1, RL95-2 cells were treated with a proteasome inhibitor, MG132. Inhibition of the proteasome degradation pathway reversed the inhibition of SP1 expression (Fig. 6F), indicating that the regulation of SP1 protein level by *O*-GlcNAcylation is a proteasome-mediated process. To further determine which residue of *O*-GlcNAcylation is critical for its stability, six putative sites were mutated to alanine ($S491^A$, $S612^A$, $T640^A$, $S641^A$, $S698^A$, $S702^A$). Results showed all mutants increased the SP1 mRNA level compared with the vector group (Fig. 6G). However, $S491^A$ did not increase but decreased AQP3 mRNA levels compared with WT (Fig. 6H), and similar results were observed at the protein level (Fig. 6I). Furthermore, $S491^A$ significantly inhibited cell proliferation (Fig. 6J) and glycolysis levels (Fig. 6K). In summary, the results showed *O*-GlcNAcylation at putative S491 affects the stability of SP1 and the transcription of AQP3.

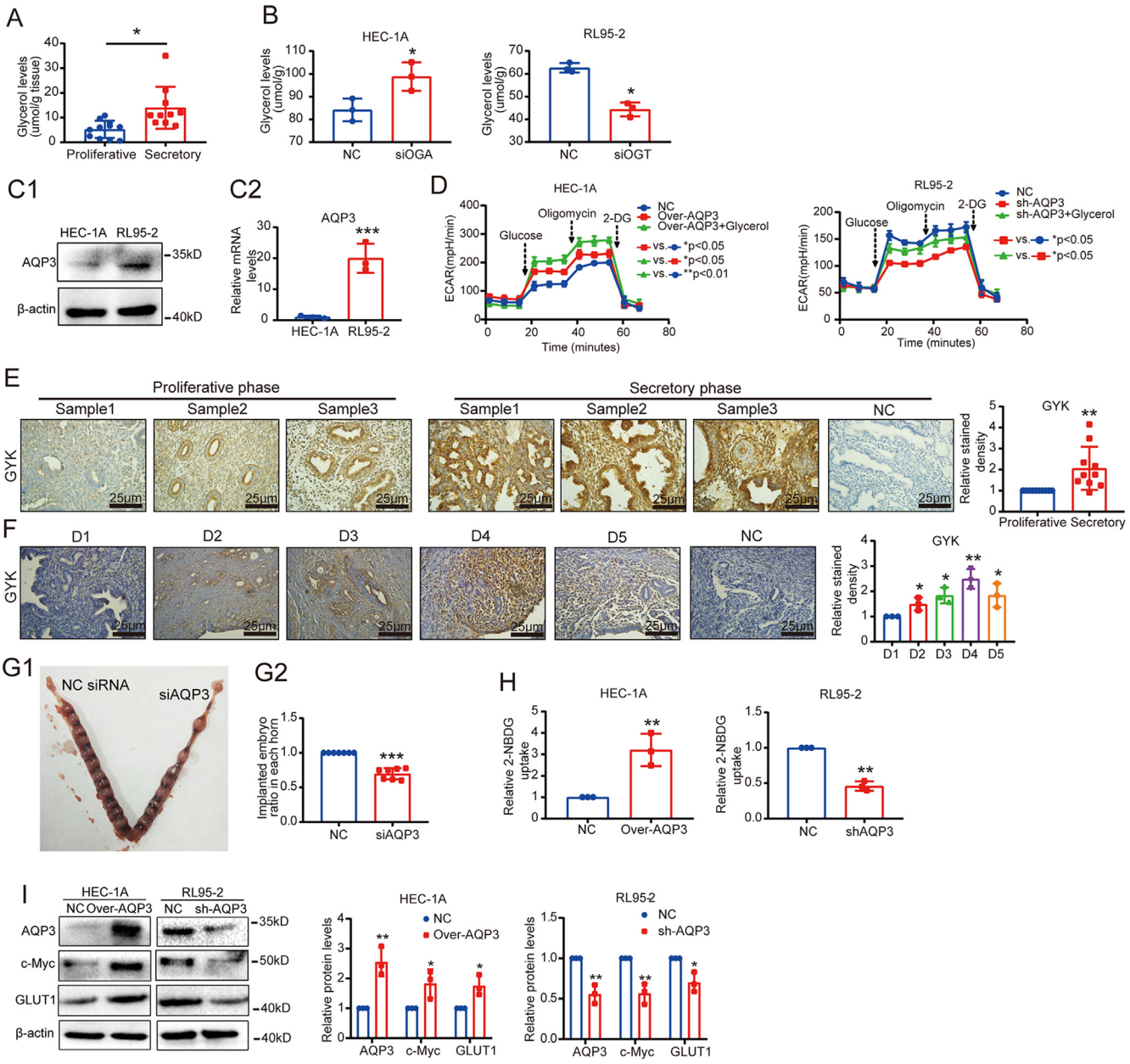

Fig. 4. AQP3 provides compensation for glycolytic metabolism. (A). Glycerol content was measured in human endometrial tissues (n = 20). (B). Glycerol content was measured in siOGA-treated HEC-1A cells or siOGT-treated RL95-2 cells (n = 3). (C1). WB analysis of AQP3 protein, and the qPCR analysis (C2) of AQP3 mRNA in HEC-1A and RL95-2 cells (normalized by β-actin; n = 3). (D). The ECAR in HEC-1A cells with empty vector, over-AQP3, over-AQP3 + glycerol (26 mM) treatments, and RL95-2 cells with empty vector, short hairpin RNA (sh)-AQP3, and sh-AQP3 + glycerol (26 mM) treatments (n = 3). (E). IHC analysis of GYK in human endometrial tissue (scale bar = 25 μm, n = 20). (F). IHC analysis of GYK expression in the uteri of mouse D1–D5 (scale bar = 25 μm, n = 3; *vs. D1). (G1). Effect of AQP3 knockdown on implantation rate with a photograph showing typical mouse uterus at D7 of pregnancy. (G2). The implanted embryo ratio in each horn was analyzed (n = 7). (H). 2-NBDG fluorescent glucose uptake assays in over-AQP3 HEC-1A and sh-AQP3 RL95-2 cells (n = 3). (I). WB analysis of AQP3, c-Myc, and GLUT1 in HEC-1A and RL95-2 cells transfected with over-AQP3 or sh-AQP3 plasmids. (n = 3; *vs. NC). Error bars represent the mean ± standard deviation. Student's *t*-test, One-way ANOVA, *P < 0.05, **P < 0.01, ***P < 0.001.

Discussion

A series of biological changes in the endometrium during embryo implantation inevitably depend on the supply of energy, and glucose metabolism is important in life processes of cell energy and material sources. In previous studies, adequate glucose uptake and metabolism were shown necessary for proper differentiation of the endometrium into the receptive state that supports embryo implantation [31]. Activated glucose metabolism promotes human decidualization [32]. Furthermore, enhanced glycolytic activity in the decidua of rodents has been verified [8,9]. However, evidence indicates that various pregnancy complications in humans are associated with abnormal glucose metabolism in the uterus, which may be the cause of poor fertility in some patients [31,33,34]. GLUT1 expression in endometrial stromal cells in patients with idiopathic infertility is reduced, indicating impaired glucose metabolism [35]. In addition, epithelial-mesenchymal transition (EMT) is involved in the opening of the epidermis after embryo attachment, and epithelial cell movement is inextricably dependent on the supply of energy [36,37]. In our two previous studies, AQP3 was shown to mediate ezrin remodeling and cytoskeletal rearrangement, affecting epithelial cell motility and participating in EMT [38]. Progesterone regulates glucose metabolism of endometrial cells through GLUT1 and affects endometrial

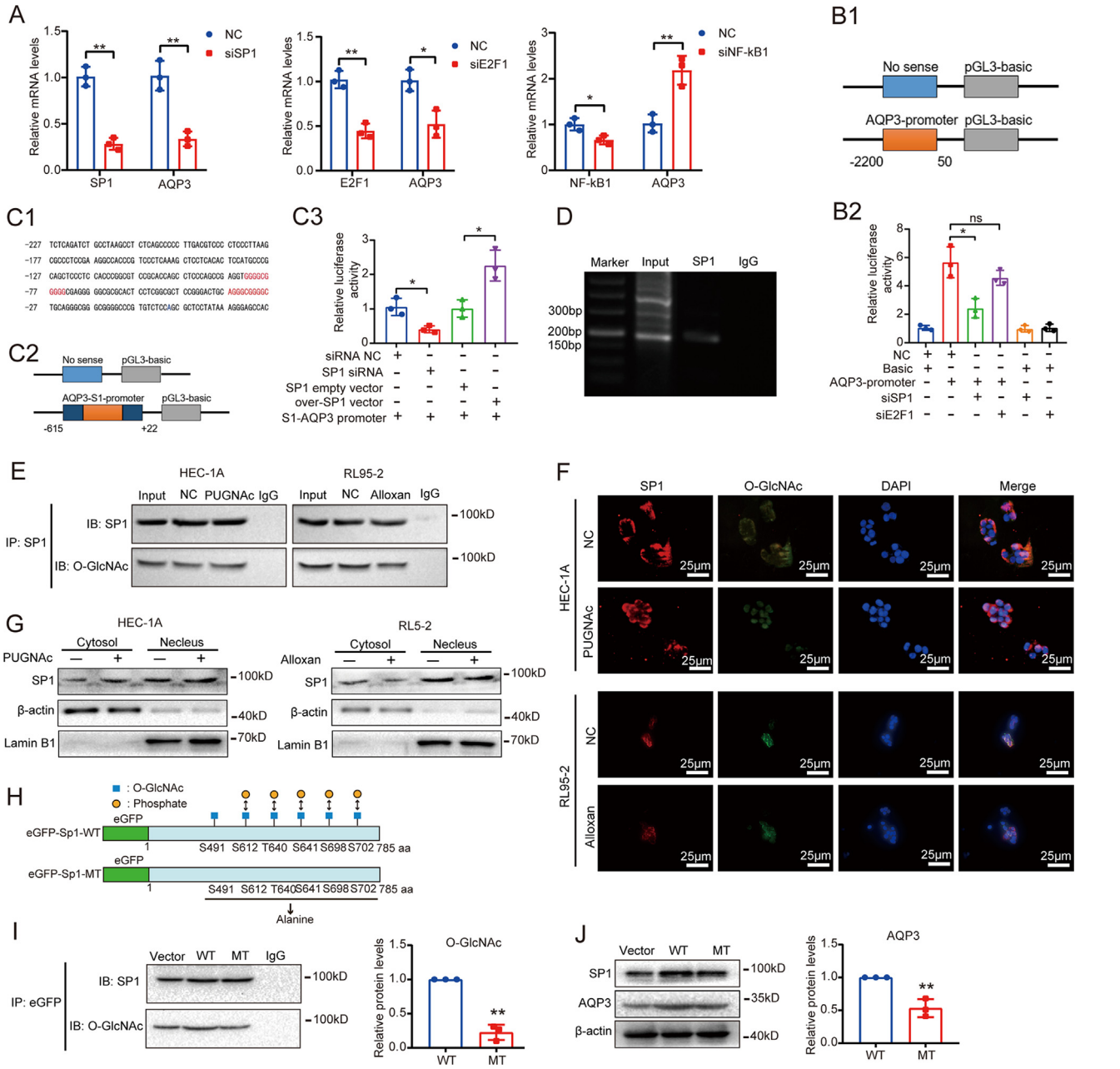

Fig. 5. The expression of AQP3 was upregulated by the *O*-GlcNAcylation of SP1. (A). qPCR analysis of AQP3 mRNA in HeLa cells transfected with siRNAs to SP1, E2F1, and NF-kB transcription factors, respectively (normalized by β-actin; n = 3). (B1). Schematic diagram of AQP3 promoter-driven luciferase reporter. (B2). A luciferase reporting system evaluated the targeting effects of HeLa cells after co-transfection with AQP3 promoter plasmids, siRNA, and scramble sequence molecules (n = 3; ns = no significant difference). (C1). Partial AQP3 promoter sequence, S1, containing predicted binding sites (two red-labeled specific binding sites). (C2). Schematic diagram of S1-driven luciferase reporter. (C3). Luciferase reporting system evaluated the targeting effects of HeLa cells after co-transfection with AQP3 promoter plasmids and over-SP1 plasmids or SP1 siRNA (n = 3). (D). ChIP analysis showed that the S1 sequence was pulled down by the anti-SP1 antibody. (E). The *O*-GlcNAcylation level was detected by WB after IP with anti-SP1 antibody in PUGNAc-treated HEC-1A cells and alloxan-treated RL95-2 cells. (F). HEC-1A cells were treated with PUGNAc and RL95-2 cells with alloxan. IF staining was performed by anti-SP1 and anti-*O*-GlcNAc (scale bar = 25 μm). (G). PUGNAc-treated HEC-1A and alloxan-treated RL95-2 cells were collected and fractionated into non-nuclear and nuclear fractions. SP1, β-actin, and lamin B1 proteins were detected by WB. (H). Schematic diagram of SP1 showing putative *O*-GlcNAc target residues that were mutagenized to alanine to generate eGFP-SP1-MT or eGFP-SP1-WT plasmids. (I). *O*-GlcNAcylation and SP1 levels were detected by WB after IP with anti-SP1 antibody in HEC-1A cells transfected with eGFP-SP1-MT or eGFP-SP1-WT plasmids (n = 3). (J). HEC-1A cells were transfected with siRNA targeting endogenous SP1 and, 24 h later, with expression plasmids for eGFP-SP1-MT and eGFP-SP1-WT. After an additional 48 h, SP1 and AQP3 proteins were then detected by WB (n = 3). Error bars represent the mean ± standard deviation. Student's *t*-test, One-way ANOVA, *P < 0.05, **P < 0.01.

receptivity [26], which indirectly implies the influence of energy metabolism/glycolysis on embryo implantation.

O-GlcNAc modification has been shown to significantly contribute to the regulation of cellular biological processes, and its role in regulating cellular metabolism has not been elucidated to date. In the present study, *O*-GlcNAcylation was shown involved in the regulation of endometrial cell function during the window of implantation, which might ensure endometrial receptivity and affect pregnancy outcome. A common phenomenon in cancer and other proliferating cells is the high rate of glucose depletion and production of lactic acid, known as the Warburg effect. These metabolic changes enable cells to obtain enough biological materi-

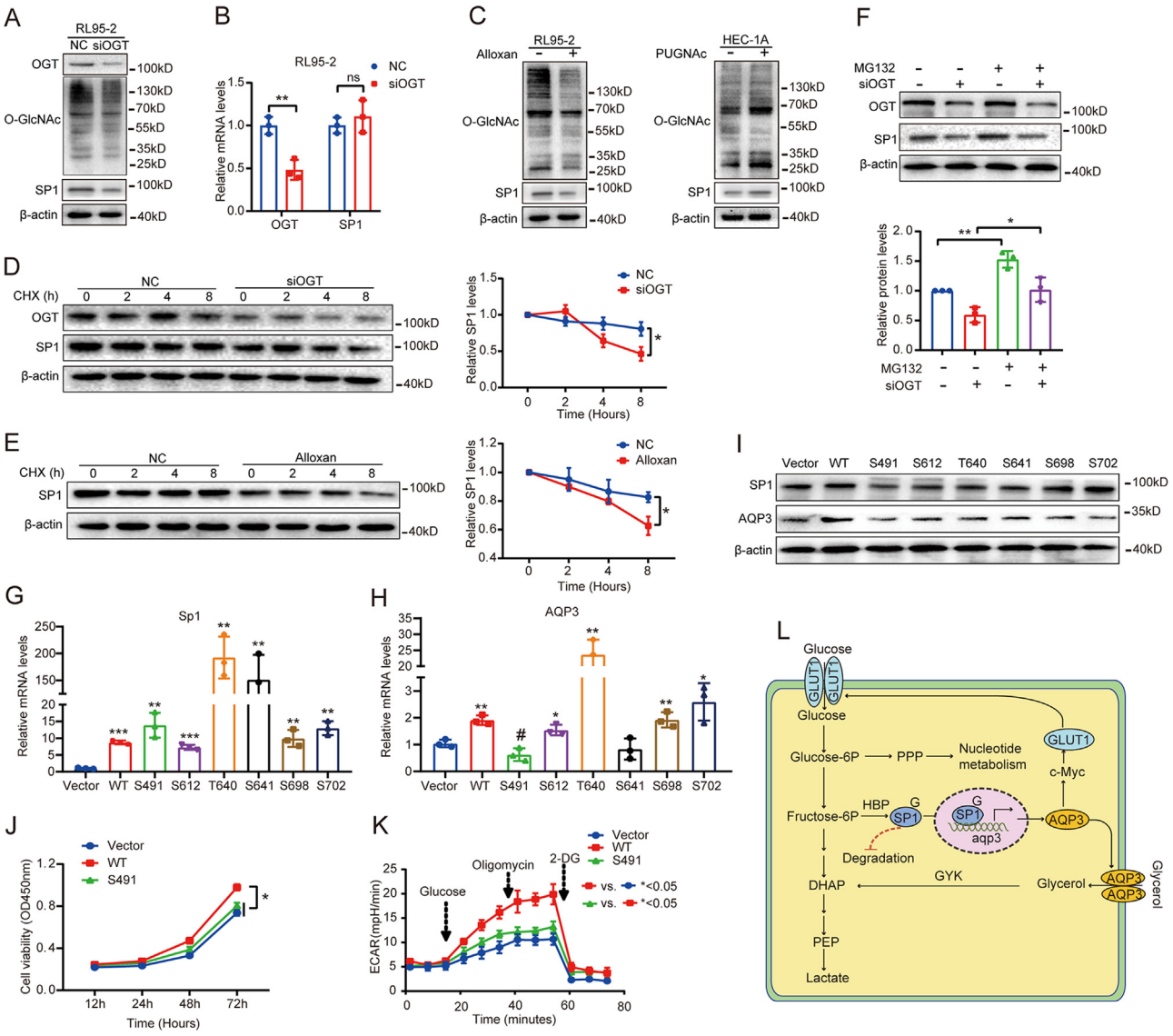

Fig. 6. The *O*-GlcNAcylation of SP1 at S491 affects its stability. (A). WB analysis of OGT, O-GlcNAcylation, and SP1 in siOGT RL95-2 cells. (B). qPCR analysis of OGT, and SP1 mRNA in siOGT RL95-2 cells (normalized by β-actin; n = 3; ns = no significant difference). (C). WB analysis of *O*-GlcNAcylation and SP1 in PUGNAc-treated HEC-1A and alloxan-treated RL95-2 cells. (D). RL95-2 cells were transfected with scrambled siRNA or siOGT for 48 h and subsequently treated with CHX (100 μM). WB analyzed OGT and SP1 proteins (n = 3). (E). RL95-2 cells were treated with DMSO control or 10 mM alloxan for 48 h and subsequently treated with CHX (100 μM). WB analyzed OGT and SP1 proteins (n = 3). (F). RL95-2 cells were transfected with NC or siOGT and were then treated with MG132 (10 μM) for 24 h. WB analyzed the OGT and SP1 (n = 3). (G-H). Sp1 (G), and AQP3 (H) mRNA levels were analyzed by qPCR in HEC-1A cells transfected with S491^A, S612^A, T640^A, S641^A, S698^A, S702^A, WT, and vector plasmids (normalized by β-actin; n = 3; *vs. vector; #vs. WT, # P < 0.05). (I). SP1 and AQP3 protein levels were analyzed by WB in HEC-1A cells transfected with S491^A, S612^A, T640^A, S641^A, S698^A, S702^A, WT, and vector plasmids. (J). Cell proliferation was measured by CCK-8 kits in HEC-1A cells transfected with S491^A, WT, and vector plasmids (n = 3). (K). ECAR of the cells was measured in HEC-1A cells transfected with S491^A, WT, and vector plasmids (n = 3). (L). A graphic model of *O*-GlcNAcylation coordinates glycolysis through GLUT1 and AQP3. Error bars represent the mean ± standard deviation. Student's *t*-test, One-way ANOVA, *P < 0.05, **P < 0.01, ***P < 0.001.

als for proper growth and differentiation to better respond to physiological needs [39,40]. Evidence shows that Warburg-like glycolysis exists in the decidualization of the endometrium [41]. In the present study, increased lactate, ATP in the secretory phase, and further enhanced cellular glycolysis were observed, indicating the Warburg-like glycolysis may also exist during the physiological change from proliferative to secretory endometrium in a receptive state and this metabolic reprogramming is regulated by *O*-GlcNAc modification.

Recently, phosphofructokinase 1 (PFK1) during glycolysis, and pyruvate kinase M2 (PKM2), which catalyzes the final glycolysis reaction, were reportedly modified by *O*-GlcNAc (i.e., *O*-GlcNAcylation inhibited their activity) [23,24], redirecting glucose metabolism to the anabolic pathway to meet the high biosynthetic demands of cells. In the present study, increased overall *O*-GlcNAc modification levels did not inhibit glycolysis but promoted it, and the limiting effect on glycolysis caused by *O*-GlcNAcylation of the enzymes could be counteracted by increased intracellular uptake of glucose. *O*-GlcNAcylation regulated glucose intake and consumption by inducing the c-Myc–mediated expression of the glycolysis-related regulator, GLUT1, which was consistent with the study by Wang *et al.* [23]. Although increased *O*-GlcNAcylation levels inhibited the activity of glycolysis-associated enzymes, it also promoted the intake of glucose by increasing GLUT1 expression, thus maintaining a higher energy supply demand for physiological changes in cells.

Transcriptome analysis also revealed *O*-GlcNAcylation regulates AQP3 expression, a member of the aquaglyceroporin family. Glyc-

erol is an important intermediate of glucose and lipid metabolism. Verkman *et al*. showed that lack of AQP3 in mice led to the slow proliferation of colonic epithelial cells due to insufficient glycerol and a low energy supply [28]. AQP7 is dynamically expressed during the decidualization of mouse endometrial cells, which leads to the accumulation of glycerol [27]. In the present study, endometrial glycerol aggregated in the secretory phase and AQP3 promoted intracellular glycerol transport and increased GYK, indicating glycerol is catalyzed to glycerol triphosphate and enters the glycolytic pathway, which may compensate for the glycolytic metabolism of endometrial cells during embryonic implantation to ensure adequate energy supply. Notably, AQP3 was found to affect glycolysis levels without glycerol as a substrate. Furthermore, AQP3 regulated glucose intake by inducing GLUT1 expression mediated by c-Myc, which provides a possible explanation for the observed phenomenon. Generally, although *O*-GlcNAcylation could redefine glucose metabolism to divert to the PPP and HBP, other pathways compensate for glycolysis, thus coordinating the overall physiological response of the cells. However, whether *O*-GlcNAc modification is involved in the metabolic changes during decidualization warrants further investigation.

To further elucidate the regulatory mechanism of *O*-GlcNAc modification regarding AQP3, SP1 was shown to specifically bind to the AQP3 promoter region to regulate AQP3 expression, and SP1 was explicitly modified by *O*-GlcNAc. In addition, the regulation of AQP3 by SP1 was influenced by its *O*-GlcNAcylation of S491. Notably, except for the S491 site, the remaining sites can be either modified by *O*-GlcNAc or phosphorylated. This peculiarity may be associated with the extensive crosstalk between *O*-GlcNAcylation and phosphorylation through the mutual inhibition of the same or adjacent residues [1,42], which warrants further investigation.

Conclusion

A series of biological changes in the endometrium during embryo implantation is closely associated with human fertility, and these changes are dependent on metabolic changes. In general, *O*-GlcNAc modification reprogramed metabolism to shunt toward the PPP and HBP during the window of implantation and compensated for glycolysis through GLUT1-mediated glucose intake and AQP3-mediated intracellular transport of glycerol (Fig. 6L), thus maintaining the physiological needs of the endometrium and regulating the receptive state of the endometrium. Therefore, the results of the present study provide new insights into the pathogenesis of metabolic disorders affecting human reproductive health.

Funding

This study was supported by the National Natural Science Foundation of China (grant no.31971209), by the Liaoning Provincial Key Research and Development Program (2019020048-JH2/10300017), Liaoning Provincial Program for Top Discipline of Basic Medical Sciences.

Compliance with Ethics Requirements

All procedures followed were in accordance with the ethical standards of the responsible committee on human experimentation (institutional and national) and with the Helsinki Declaration of 1975, as revised in 2008 (5). Informed consent was obtained from all patients for being included in the study.

Compliance with Ethics Requirements

All Institutional and National Guidelines for the care and use of animals (fisheries) were followed.

Availability of data and materials

The transcriptome-sequencing data is available from the Sequence Read Archive (https://dataview.ncbi.nlm.nih.gov/object/PRJNA663732?reviewer=oqoo23cjr4f6ue637n08q2epb7). All Original/source data for figures in the paper is available on request to the corresponding author.

CRediT authorship contribution statement

Hongshuo Zhang: Writing - original draft, Visualization. **Jia Qi:** Visualization, Investigation. **Jingyuan Pei:** Investigation. **Man Zhang:** Investigation. **Yuhong Shang:** Investigation. **Zhen Li:** Investigation. **Yufei Wang:** Investigation. **Jinqiu Guo:** Validation. **Kaiqi Sun:** Validation. **Jianhui Fan:** Writing - review & editing. **Linlin Sui:** Writing - review & editing. **Yuefei Xu:** Writing - review & editing. **Li Kong:** Conceptualization, Supervision. **Ying Kong:** Conceptualization, Funding acquisition.

Declaration of Competing Interest

The authors declare that they have no known competing financial interests or personal relationships that could have appeared to influence the work reported in this paper.

Appendix A. Supplementary data

Supplementary data to this article can be found online at https://doi.org/10.1016/j.jare.2021.06.022.

References

[1] Hu P, Shimoji S, Hart GW. Site-specific interplay between O-GlcNAcylation and phosphorylation in cellular regulation. FEBS Lett 2010;584(12):2526–38.
[2] Zeidan Q, Hart GW. The intersections between O-GlcNAcylation and phosphorylation: implications for multiple signaling pathways. J Cell Sci 2010;123(Pt 1):13–22.
[3] Butkinaree C, Park K, Hart GW. O-linked beta-N-acetylglucosamine (O-GlcNAc): Extensive crosstalk with phosphorylation to regulate signaling and transcription in response to nutrients and stress. Biochim Biophys Acta 2010;1800(2):96–106.
[4] Caldwell SA, Jackson SR, Shahriari KS, Lynch TP, Sethi G, Walker S, et al. Nutrient sensor O-GlcNAc transferase regulates breast cancer tumorigenesis through targeting of the oncogenic transcription factor FoxM1. Oncogene 2010;29(19):2831–42.
[5] Teh WT, McBain J, Rogers P. What is the contribution of embryo-endometrial asynchrony to implantation failure. J Assist Reprod Genet 2016;33(11):1419–30.
[6] Wang H, Dey SK. Roadmap to embryo implantation: clues from mouse models. Nat Rev Genet 2006;7(3):185–99.
[7] Cha J, Sun X, Dey SK. Mechanisms of implantation: strategies for successful pregnancy. Nat Med 2012;18(12):1754–67.
[8] Murdoch RN. Glycolysis in the mouse uterus during the early post-implantation stages of pregnancy and the effects of acute doses of ethanol. Teratology 1987;35(2):169–76.
[9] Surani MA, Heald PJ. Changes in enzymes of carbohydrate metabolism in rat uterus during early pregnancy. Acta Endocrinol (Copenh) 1971;68(4):805–16.
[10] Slawson C, Copeland RJ, Hart GW. O-GlcNAc signaling: a metabolic link between diabetes and cancer. Trends Biochem Sci 2010;35(10):547–55.
[11] Ruan YC, Guo JH, Liu X, Zhang R, Tsang LL, Dong JD, et al. Activation of the epithelial Na+ channel triggers prostaglandin E_2 release and production required for embryo implantation. Nat Med 2012;18(7):1112–7.
[12] Sun X, Ruan YC, Guo J, Chen H, Tsang LL, Zhang X, et al. Regulation of miR-101/miR-199a-3p by the epithelial sodium channel during embryo implantation: involvement of CREB phosphorylation. Reproduction 2014;148(6):559–68.
[13] Dominguez F, Galan A, Martin JJ, Remohi J, Pellicer A, Simón C. Hormonal and embryonic regulation of chemokine receptors CXCR1, CXCR4, CCR5 and CCR2B in the human endometrium and the human blastocyst. Mol Hum Reprod 2003;9(4):189–98.
[14] Hannan NJ, Paiva P, Dimitriadis E, Salamonsen LA. Models for study of human embryo implantation: choice of cell lines. Biol Reprod 2010;82(2):235–45.
[15] Hohn HP, Linke M, Denker HW. Adhesion of trophoblast to uterine epithelium as related to the state of trophoblast differentiation: in vitro studies using cell lines. Mol Reprod Dev 2000;57(2):135–45.
[16] Bacigalupa ZA, Bhadiadra CH, Reginato MJ. O-GlcNAcylation: key regulator of glycolytic pathways. J Bioenerg Biomembr 2018;50(3):189–98.

[17] Kommaddi RP, Dickson KM, Barker PA. Stress-induced expression of the p75 neurotrophin receptor is regulated by O-GlcNAcylation of the Sp1 transcription factor. J Neurochem 2011;116(3):396–405.
[18] Lee HJ, Ryu JM, Jung YH, Lee KH, Kim DI, Han HJ. Glycerol-3-phosphate acyltransferase-1 upregulation by O-GlcNAcylation of Sp1 protects against hypoxia-induced mouse embryonic stem cell apoptosis via mTOR activation. Cell Death Dis 2016;7:e2158.
[19] Godbole GB, Modi DN, Puri CP. Regulation of homeobox A10 expression in the primate endometrium by progesterone and embryonic stimuli. Reproduction 2007;134(3):513–23.
[20] Modi D, Godbole G. HOXA10 signals on the highway through pregnancy. J Reprod Immunol 2009;83(1–2):72–8.
[21] Lee TN, Alborn WE, Knierman MD, Konrad RJ. Alloxan is an inhibitor of O-GlcNAc-selective N-acetyl-beta-D-glucosaminidase. Biochem Biophys Res Commun 2006;350(4):1038–43.
[22] Whitworth GE, Macauley MS, Stubbs KA, Dennis RJ, Taylor EJ, Davies GJ, et al. Analysis of PUGNAc and NAG-thiazoline as transition state analogues for human O-GlcNAcase: mechanistic and structural insights into inhibitor selectivity and transition state poise. J Am Chem Soc 2007;129(3):635–44.
[23] Wang Y, Liu J, Jin X, Zhang D, Li D, Hao F, et al. O-GlcNAcylation destabilizes the active tetrameric PKM2 to promote the Warburg effect. Proc Natl Acad Sci U S A 2017;114(52):13732–7.
[24] Yi W, Clark PM, Mason DE, Keenan MC, Hill C, Goddard WA, et al. Phosphofructokinase 1 glycosylation regulates cell growth and metabolism. Science 2012;337(6097):975–80.
[25] Ferrer CM, Lynch TP, Sodi VL, Falcone JN, Schwab LP, Peacock DL, et al. O-GlcNAcylation regulates cancer metabolism and survival stress signaling via regulation of the HIF-1 pathway. Mol Cell 2014;54(5):820–31.
[26] Zhang H, Qi J, Wang Y, Sun J, Li Z, Sui L, et al. Progesterone Regulates Glucose Metabolism Through Glucose Transporter 1 to Promote Endometrial Receptivity. Front Physiol 2020;11:543148.
[27] Peng H, Zhang Y, Lei L, Chen Q, Yue J, Tan Y, et al. Aquaporin 7 expression in postimplantation mouse uteri: a potential role for glycerol transport in uterine decidualization. Fertil Steril 2011;95(4). pp. 1514–7.e1-3.
[28] Thiagarajah JR, Zhao D, Verkman AS. Impaired enterocyte proliferation in aquaporin-3 deficiency in mouse models of colitis. Gut 2007;56(11):1529–35.
[29] Zhu N, Feng X, He C, Gao H, Yang L, Ma Q, et al. Defective macrophage function in aquaporin-3 deficiency. FASEB J 2011;25(12):4233–9.
[30] Jackson SP, Tjian R. O-glycosylation of eukaryotic transcription factors: implications for mechanisms of transcriptional regulation. Cell 1988;55(1):125–33.
[31] Frolova AI, Moley KH. Glucose transporters in the uterus: an analysis of tissue distribution and proposed physiological roles. Reproduction 2011;142(2):211–20.
[32] Kommagani R, Szwarc MM, Kovanci E, Gibbons WE, Putluri N, Maity S, et al. Acceleration of the glycolytic flux by steroid receptor coactivator-2 is essential for endometrial decidualization. PLoS Genet 2013;9(10):e1003900.
[33] Hackl H. Metabolism of glucose in the human endometrium with special reference to fertility and contraception. Acta Obstet Gynecol Scand 1973;52(2):135–40.
[34] Kim JY, Song H, Kim H, Kang HJ, Jun JH, Hong SR, et al. Transcriptional profiling with a pathway-oriented analysis identifies dysregulated molecular phenotypes in the endometrium of patients with polycystic ovary syndrome. J Clin Endocrinol Metab 2009;94(4):1416–26.
[35] von Wolff M, Ursel S, Hahn U, Steldinger R, Strowitzki T. Glucose transporter proteins (GLUT) in human endometrium: expression, regulation, and function throughout the menstrual cycle and in early pregnancy. J Clin Endocrinol Metab 2003;88(8):3885–92.
[36] Uchida H, Maruyama T, Nishikawa-Uchida S, Oda H, Miyazaki K, Yamasaki A, et al. Studies using an in vitro model show evidence of involvement of epithelial-mesenchymal transition of human endometrial epithelial cells in human embryo implantation. J Biol Chem 2012;287(7):4441–50.
[37] Owusu-Akyaw A, Krishnamoorthy K, Goldsmith LT, Morelli SS. The role of mesenchymal-epithelial transition in endometrial function. Hum Reprod Update 2019;25(1):114–33.
[38] Cui D, Sui L, Han X, Zhang M, Guo Z, Chen W, et al. Aquaporin-3 mediates ovarian steroid hormone-induced motility of endometrial epithelial cells. Hum Reprod 2018;33(11):2060–73.
[39] Intlekofer AM, Finley L. Metabolic signatures of cancer cells and stem cells. Nat Metab 2019;1(2):177–88.
[40] Schwörer S, Vardhana SA, Thompson CB. Cancer Metabolism Drives a Stromal Regenerative Response. Cell Metab 2019;29(3):576–91.
[41] Zuo RJ, Gu XW, Qi QR, Wang TS, Zhao XY, Liu JL, et al. Warburg-like Glycolysis and Lactate Shuttle in Mouse Decidua during Early Pregnancy. J Biol Chem 2015;290(35):21280–91.
[42] Zhao L, Shah JA, Cai Y, Jin J. 'O-GlcNAc Code' Mediated Biological Functions of Downstream Proteins. Molecules 2018;23(8).